

Interfacial Behavior of Cholesterol, Ergosterol, and Lanosterol in Mixtures with DPPC and DMPC

Karen Sabatini, Juha-Pekka Mattila, and Paavo K. J. Kinnunen

Helsinki Biophysics and Biomembrane Group, Medical Biochemistry, Institute of Biomedicine, FIN-00014 University of Helsinki, Finland

ABSTRACT Binary mixtures of cholesterol, ergosterol, and lanosterol with phosphatidylcholines differing in the length of the saturated acyl chains, viz 1,2-dipalmitoyl-*sn*-glycero-3-phosphocholine (DPPC) and 1-palmitoyl-2-myristoyl-*sn*-glycero-3-phosphocholine (DMPC), were analyzed using a Langmuir balance for recording force-area (π - A) and surface potential-area (ψ - A) isotherms. A progressive disappearance of the liquid expanded–liquid condensed transition was observed in mixed monolayers with DPPC after the increase in the content of all three sterols. For fluid DMPC matrix, no modulation of the monolayer phase behavior due to the sterols was evident with the exception of lanosterol, for which a pronounced discontinuity between mole fractions of $X = 0.3$ and $X = 0.75$ was discernible in the compression isotherms. Condensing and expanding effects in force-area (π - A) isotherms due to varying X_{sterols} and differences in the monolayer physical state were assessed from the values for the interfacial compression moduli. Surface potential measurements support the notion that cholesterol and ergosterol, but not lanosterol, reduce the penetration of water into the lipid monolayers. Examination of the excess free energy of mixing revealed an enhanced stability of binary monolayers containing cholesterol compared to those with ergosterol or lanosterol; the differences are emphasized in the range of surface pressure values found in natural membranes.

INTRODUCTION

Sterols are complex molecules representing the products of a long biochemical evolution (1–3) and are abundant constituents of membranes of plant and animal cells (4–7). In contrast to the high diversity in the phospholipid composition of the different cellular membranes in the different species, there is significantly less variation in sterol structures. Cholesterol is abundant in the membranes of higher eukaryotes and is essential for their integrity, organization, and function. Ergosterol is found in lower eukaryotes: some protozoa, yeast, fungi, and insects such as *Drosophila* (3,7,8). Lanosterol is a constituent of prokaryotic cell membranes, and it is the common biosynthetic precursor in both cholesterol and ergosterol pathways (7–11). It emerged for the first time in an aerobic environment and has been suggested to represent a “living molecular fossil”, which is considered to be the evolutionary precursor of sterols (1,8,10,12–15).

Sterols influence the conformational order of the lipid acyl chains (4,9,10,16) and membrane permeability (10). Further, sterols regulate the membrane lateral organization (9,17) and the membrane hydrophobic thickness that is responsible in part for the regulation of lipid-protein interactions (9,18,19). Sterols, in particular cholesterol, have cohesive interactions with saturated lipids (4,20,21) and, in general, the degree of lipid unsaturation influences sterol-lipid packing and consequently membrane properties (2,9,11,20,21). Cholesterol, lanosterol, and ergosterol (Fig. 1) have similar dimensions,

including the length of the rigid ring and the total length of the molecule (9), and they share common features including a planar cyclopentane-phenantrene ring, a 3β -OH group, and a hydrophobic side chain linked to C_{17} (2). Yet, there are also distinct structural differences that are the basis for their different behaviors with respect to interactions with other lipids and modulation of membrane properties (2,4,11,13,17). Cholesterol has two β -oriented methyl groups at C_{10} and C_{13} and a branched hydrocarbon tail at C_{17} . Cholesterol orients itself with its 3β -OH group in proximity to the phospholipid ester carbonyl oxygen, within the hydrophobic-hydrophilic interface, and aligns its long molecular axis parallel with the acyl chains of membrane phospholipids. Thus, the interaction between the rigid and smooth hydrophobic part of cholesterol, as well as its side chain and other lipid species, is due to van der Waals forces and is inherent to the cholesterol structure itself. Ergosterol differs from cholesterol in having two additional double bonds, one in the rigid ring at position C_7 and the other in its tail at C_{22} , and an additional methyl group on the side chain at C_{24} . The presence of the double bond in the ring has been suggested to increase its interactions with phospholipid acyl chains due to enhanced van der Waals forces, increasing the planarity of the ring (4). Lanosterol has three additional methyl groups compared to cholesterol, two of which are attached to C_4 (α - and β -faces) and the third attached to C_{14} (α -face), thus making the α -face asymmetric. Moreover, lanosterol contains two double bonds, one at position C_8 and the second at position C_{24} . Because of the three additional methyl groups, lanosterol is bulkier than cholesterol, and its structure does not facilitate strong interactions with lipids. Also in the case of lanosterol, as well as for ergosterol, the amphiphilic nature of these molecules orients them with their hydrophobic part

Submitted February 22, 2008, and accepted for publication May 16, 2008.

Address reprint requests to Paavo K. J. Kinnunen, Helsinki Biophysics and Biomembrane Group Medical Biochemistry, Institute of Biomedicine, PO Box 63 (Haartmaninkatu 8), FIN-00014 University of Helsinki, Finland. Fax: 358-0-191 25444; E-mail: paavo.kinnunen@helsinki.fi.

Editor: Thomas J. McIntosh.

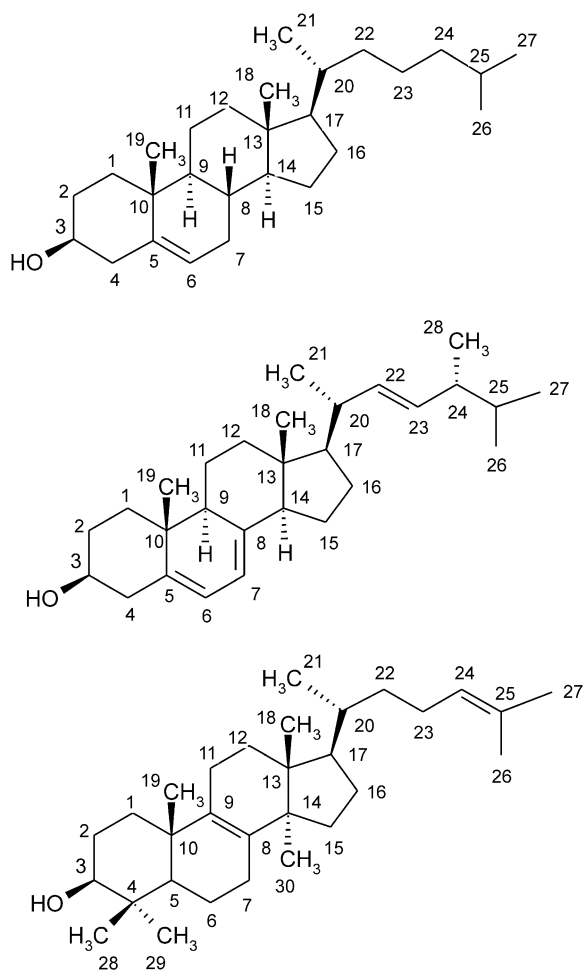


FIGURE 1 Chemical structures of the three sterols used. (Top to bottom) β -cholesterol, ergosterol, and lanosterol.

between the lipid acyl chains and with the hydroxyl group close to the phospholipid ester carbonyl oxygen.

As mentioned above, cholesterol, ergosterol, and lanosterol represent the most important and common sterols in different kingdoms. To further elucidate how these three sterols modify the biophysical properties of biologic membranes, we used a Langmuir balance to analyze their effects on DPPC and DMPC monolayers. The former lipid exhibits the thoroughly characterized phase transition from the liquid condensed (LC) to liquid expanded (LE) state, whereas for the latter the LE state prevails throughout the whole range of surface pressures reached during compression. Notably, unsaturated phospholipids were not used because the presence of double bond(s) influences the sterol-lipid packing and consequently membrane properties (2,9,11,20). Accordingly, this approach allowed us to focus solely on the influence of phase behavior on the interactions between the sterols and phospholipids, investigated by recording force-area (π - A) isotherms and calculating from these data the interfacial elastic moduli of area compressibility (C_s^{-1}), providing an indicator for changes in the structure of the film (22). Infor-

mation on the electric properties of the film was obtained from the measurement of surface dipole potential ψ (23). The thermodynamic stability of mixed monolayers was investigated analyzing the excess free energy of mixing ($\Delta G_{\text{mix}}^{\text{exc}}$).

MATERIALS AND METHODS

Materials

1-Palmitoyl-2-myristoyl-*sn*-glycero-3-phosphocholine (DMPC), β -cholesterol, lanosterol and NaCl were purchased from Sigma (St. Louis, MO), 1,2-dipalmitoyl-*sn*-glycero-3-phosphocholine (DPPC) from Avanti Polar Lipids (Alabaster, AL), and ergosterol from Fluka (Neu-Ulm, Germany). The purity of the above lipids was verified by thin layer chromatography on silicic acid-coated plates (Merck, Darmstadt, Germany), using chloroform/methanol/water/ammonia (65:20:2:2, v/v) as the eluent. No impurities were detected upon examination of the plates after iodine staining. Concentrations of DPPC, DMPC, β -cholesterol, lanosterol, and ergosterol were determined gravimetrically using a high-precision electrobalance (Cahn Instruments, Cerritos, CA). Stock solutions of the lipids were prepared in chloroform and stored at -20°C . Freshly deionized filtered water (Milli RO/Milli Q; Millipore, Jaffrey, NH) was used in all experiments.

Monolayer measurements

A computer-controlled Langmuir type film balance (μ Trough XL; Kibron, Helsinki, Finland) equipped with a Precision Plus trough (Kibron) was used to simultaneously measure π - A and surface potential-area ($\Delta\psi$ - A) isotherms, using the embedded features of the control software (FilmWare 3.57; Kibron). The indicated lipid mixtures were made in chloroform and were spread in this solvent onto the air-aqueous phase (15 mM NaCl) interface with a microsyringe (Hamilton, Reno, NV). This subphase was used because the presence of salt decreases noise in the surface potential measurements. The total surface area of the trough was 120 cm^2 , and the volume of the subphase was 40 ml. After 5 min equilibration (to ensure evaporation of the solvent), film compression was started using two symmetrically moving barriers. In all measurements, the compression rate was $4\text{ \AA}^2/\text{chain}/\text{min}$ to allow for the reorientation and relaxation of the lipids in the course of the compression. Surface pressure (π) was monitored with a metal alloy probe hanging from a high precision microbalance (KBN 315; Kibron) connected to a computer and is defined as follows:

$$\pi = \gamma_o - \gamma, \quad (1)$$

where γ_o is the surface tension of the air/buffer interface and γ is the value for surface tension in the presence of a lipid monolayer compressed to varying packing densities. Monolayer dipole potential ψ (23) was measured using the vibrating plate method (μ Spot; Kibron). All isotherms were recorded at ambient temperature ($\sim 23^\circ\text{C}$) and were repeated at least twice to ensure reproducibility. Importantly, oxidation of cholesterol included in DMPC monolayers has been shown to an observable extent only after ~ 30 – 40 min of air exposure (24), whereas our experiments generally last ~ 20 min. Moreover, it has been demonstrated that cholesterol oxidation is not responsible for the observed transformation of nanodomains to microdomains after exposition of monolayers to air (25). Hence, although lack of sterol oxidation cannot be excluded, its effects should not contribute to our results.

Analysis of isotherms

Phase transitions were identified using derivatives of surface pressure with respect to area (26). The value for monolayer isothermal compressibilities (C_s) for the indicated film compositions at the given surface pressure (π) was obtained from π - A data as follows:

$$C_s = (-1/A_\pi) \times (dA/d\pi)_T, \quad (2)$$

where A_π is the area per molecule at the indicated surface pressure π . To identify the phase transition points, we further analyzed our data in terms of the reciprocal isothermal compressibility (C_s^{-1}), as discussed previously (27). Accordingly, the higher the value is for the compressibility modulus C_s^{-1} , the lower the interfacial elasticity will be.

The collected $\Delta\psi$ - A data were analyzed in terms of μ_\perp —the component of the monolayer dipole moment vector perpendicular to the monolayer plane. The values for μ_\perp were obtained essentially as described by Brockman (23). In brief, $\Delta\psi$ was plotted against $1/A_m$ and subsequently the curves were fitted by the equation as follows:

$$\Delta\psi = \Delta\psi_0 + 37.70 \mu_\perp \times 1/A_m \quad (3)$$

to yield an estimate of molecular dipole moment μ_\perp . $\Delta G_{\text{mix}}^{\text{exc}}$, the excess free energy of mixing, was calculated as the compression work difference between ideal and real monolayer mixtures from the experimental π - A isotherms using the equation as follows:

$$\Delta G_{\text{mix}}^{\text{exc}} = \int_0^\pi A - X_1 A_1 - X_2 A_2 d\pi, \quad (4)$$

where A is the measured area/molecule value for binary monolayer and X_n and A_n represent the mole fraction and area/molecule value of the n th monolayer component at given π , respectively (28,29).

RESULTS

π - A isotherms for sterols in mixed monolayers with DPPC and DMPC

We first recorded compression isotherms for pure sterols (Fig. 2). Compared to cholesterol, in which the isotherm starts to raise sharply around $37 \text{ \AA}^2/\text{molecule}$, higher lift-off values were evident for ergosterol and lanosterol ($\sim 45 \text{ \AA}^2/\text{molecule}$ and $\sim 50 \text{ \AA}^2/\text{molecule}$, respectively). This observation likely reflects the bulkier structures of the latter two sterols arising from the additional methyl groups and side-chain double bonds, manifesting as reduced packing effectiveness, increased tilt of the molecules with respect to the monolayer plane, and augmented penetration of water into the monolayer. In addition, the presence of the double bond reduces the hydrophobicity of the branched hydrocarbon tail of ergosterol and lanosterol, which could cause these sterols to have their long axis parallel to the interface. Deviating from both cholesterol and ergosterol at ~ 31 – 32 mN/m and at $\sim 27 \text{ \AA}^2/\text{molecule}$, the isotherm of lanosterol starts to bend. Beyond this point, the surface pressure continues to increase without a discernible film collapse in the π - A data. DPPC formed stable monolayers, and its compression isotherm revealed a clear LE to LC (LE \rightarrow LC) main phase transition, as reported previously (30).

We subsequently recorded π - A isotherms of DPPC with cholesterol, ergosterol, and lanosterol (Fig. 2). Analysis of these data revealed several interesting features. First, increasing X_{sterol} results in the progressive disappearance of the

LE-LC coexistence region. More specifically, films with $X_{\text{sterol}} = 0.1$ still preserve the LE-LC transition, although it is narrow and appears at lower area/molecule value compared to neat DPPC, in keeping with the condensing effect of sterols (31). Moreover, it appears at different values of π for the different sterols: for cholesterol, a lower value is evident than for pure DPPC, whereas the opposite is true for ergosterol and lanosterol. For cholesterol and ergosterol with $X_{\text{sterol}} \geq 0.3$ the coexistence region is no more seen, whereas monolayers with similar amounts of lanosterol still preserve the LE-LC coexistence, albeit at different values of π .

The second interesting feature of the isotherms is the different condensing effect of the three sterols. Upon increase of X_{sterol} , the compression isotherms lift-off at smaller area/molecule. Films with $X_{\text{chol}} = 0.1, 0.3, 0.5,$ and 0.75 lift-off at ~ 18 – $20, \sim 40, \sim 57,$ and $\sim 61 \text{ \AA}^2$ smaller area/molecule, respectively, compared to pure DPPC. For ergosterol, this difference is $\sim 15 \text{ \AA}^2$ at $X_{\text{ergo}} = 0.1$ and $\sim 25 \text{ \AA}^2$ at $X_{\text{ergo}} = 0.3$; for lanosterol, it is $\sim 5 \text{ \AA}^2$ at $X_{\text{lano}} = 0.1$ and $\sim 20 \text{ \AA}^2$ for $X_{\text{lano}} = 0.3$. For both ergosterol and lanosterol at $X_{\text{sterol}} = 0.5$, the difference is $\sim 40 \text{ \AA}^2$ and $\sim 50 \text{ \AA}^2$ for $X_{\text{sterol}} = 0.75$. To further investigate the condensing and expanding effects due to the sterols, we analyzed the isobars of mean molecular area \bar{A} vs. X_{sterol} at surface pressures of 5, 10, 20, 30, and 40 mN/m (Fig. 3, A–C). In the LE state at 5 mN/m, all three sterols induce a film condensation, which is most pronounced for cholesterol. For the whole range of analyzed pressures and for all compositions, cholesterol produces a clear condensation (Fig. 3 A), whereas ergosterol induces a slight condensation from pressure of 20 up to 40 mN/m below $X_{\text{ergo}} = 0.75$, where the miscibility is close to ideal. An interesting feature is evident for ergosterol at the $\pi = 10 \text{ mN/m}$ where $X_{\text{ergo}} = 0.1$ and 0.3 both produce a slight expansion of the film (Fig. 3 B). This behavior is also seen for lanosterol with a more pronounced expansion of the film at $X_{\text{lano}} = 0.75$, especially at surface pressures between 30 and 40 mN/m, and at $X_{\text{lano}} = 0.5$ at high surface pressures (40 mN/m) (Fig. 3 C).

We then studied binary mixtures of the sterols and DMPC. The compression isotherms for this phospholipid in binary mixtures with cholesterol and ergosterol reveal an LE state at all surface pressures below the monolayer collapse. Notably, and contrary to all the other films (including that of $X_{\text{lano}} = 0.1$) in which there are no indications of discontinuities, a shoulder appears at π below 10 mN/m in the isotherm for $X_{\text{lano}} = 0.3$. This shoulder shifts to higher pressures for films with $X_{\text{lano}} = 0.5$ and 0.75 .

For the whole range of analyzed pressures and all mole fractions, the \bar{A} vs. X_{sterol} data at 5, 10, 20, 30, and 40 mN/m show the condensing effect of cholesterol in DMPC monolayers, with the sole exception of $X_{\text{chol}} = 0.75$ at $\pi = 40 \text{ mN/m}$ where a slight expansion is seen (Fig. 3 D). A condensing effect is seen also for ergosterol and lanosterol even though it is less pronounced compared to cholesterol (Fig. 3 E). In addition, lanosterol causes a clear expansion at 40 mN/m for films with $X_{\text{lano}} = 0.5$ and 0.75 (Fig. 3 F).

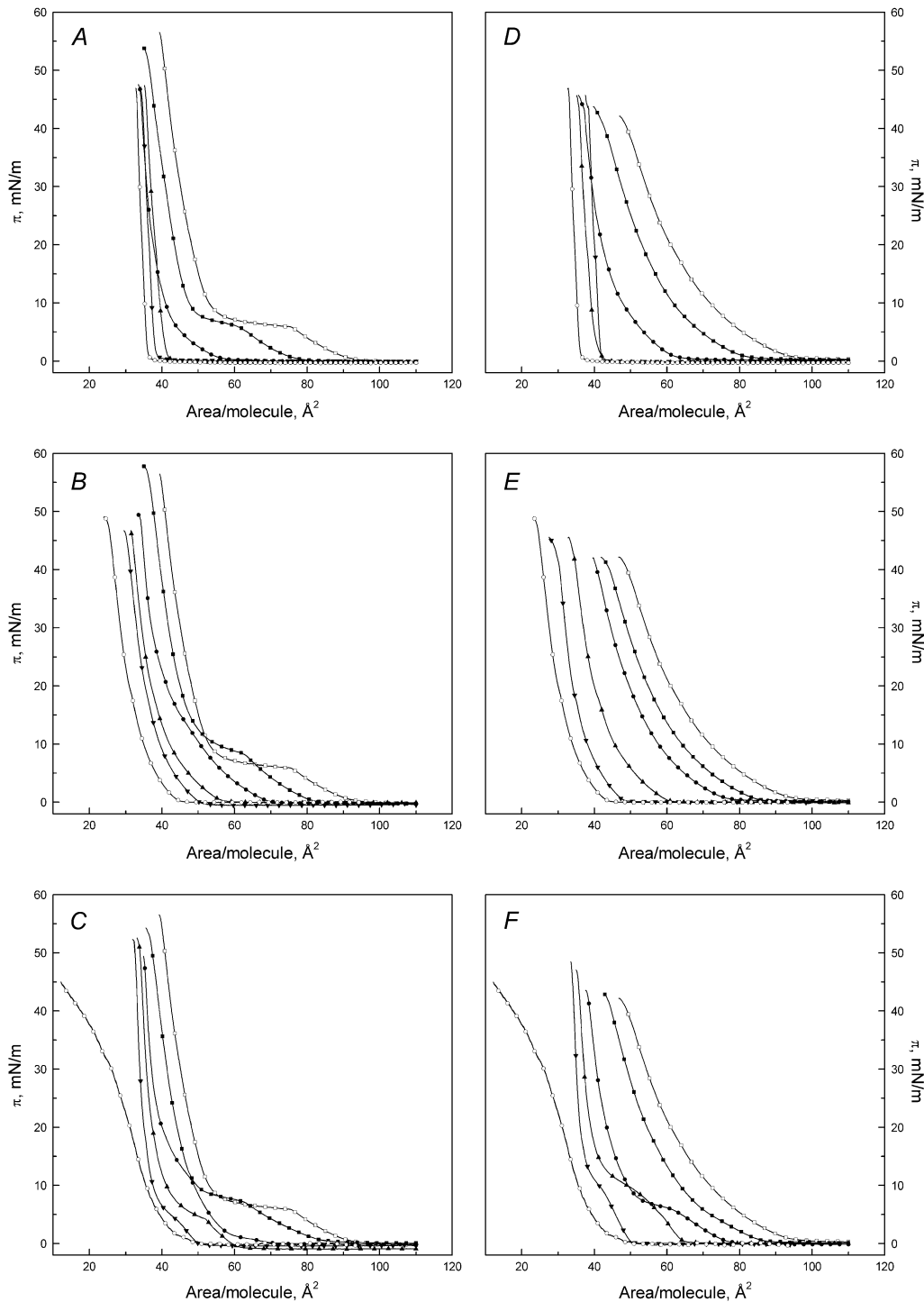


FIGURE 2 Representative compression isotherms for cholesterol (*A* and *D*), ergosterol (*B* and *E*), and lanosterol (*C* and *F*) in mixed monolayers with DPPC (*left*) and DMPC (*right*), the mole fraction of the sterols (X_{sterols}) increasing from right to left as 0.0 (\square), 0.1 (\blacksquare), 0.3 (\bullet), 0.5 (\blacktriangle), 0.75 (\blacktriangledown), and 1.0 (\circ). The given lipid mixtures were spread onto 15 mM NaCl at ambient temperature ($\sim 24^\circ\text{C}$). After 4 min of equilibration, the films were compressed at a rate of $4 \text{ \AA}^2/\text{molecule}/\text{min}$. Standard deviations would be contained within the symbols and were omitted for clarity.

Interfacial elastic moduli of area compressibility

The compressibility modulus C_s^{-1} , reflecting variations in the physical state of the films, was calculated as a function of π and X_{sterol} from the π - A compression isotherms. The analysis

of pure sterols reveals that cholesterol displays the highest value of C_s^{-1} followed by ergosterol and lanosterol. For the latter, it is of interest that starting from $\pi \approx 17 \text{ mN/m}$, the values of C_s^{-1} decrease with increasing pressure.

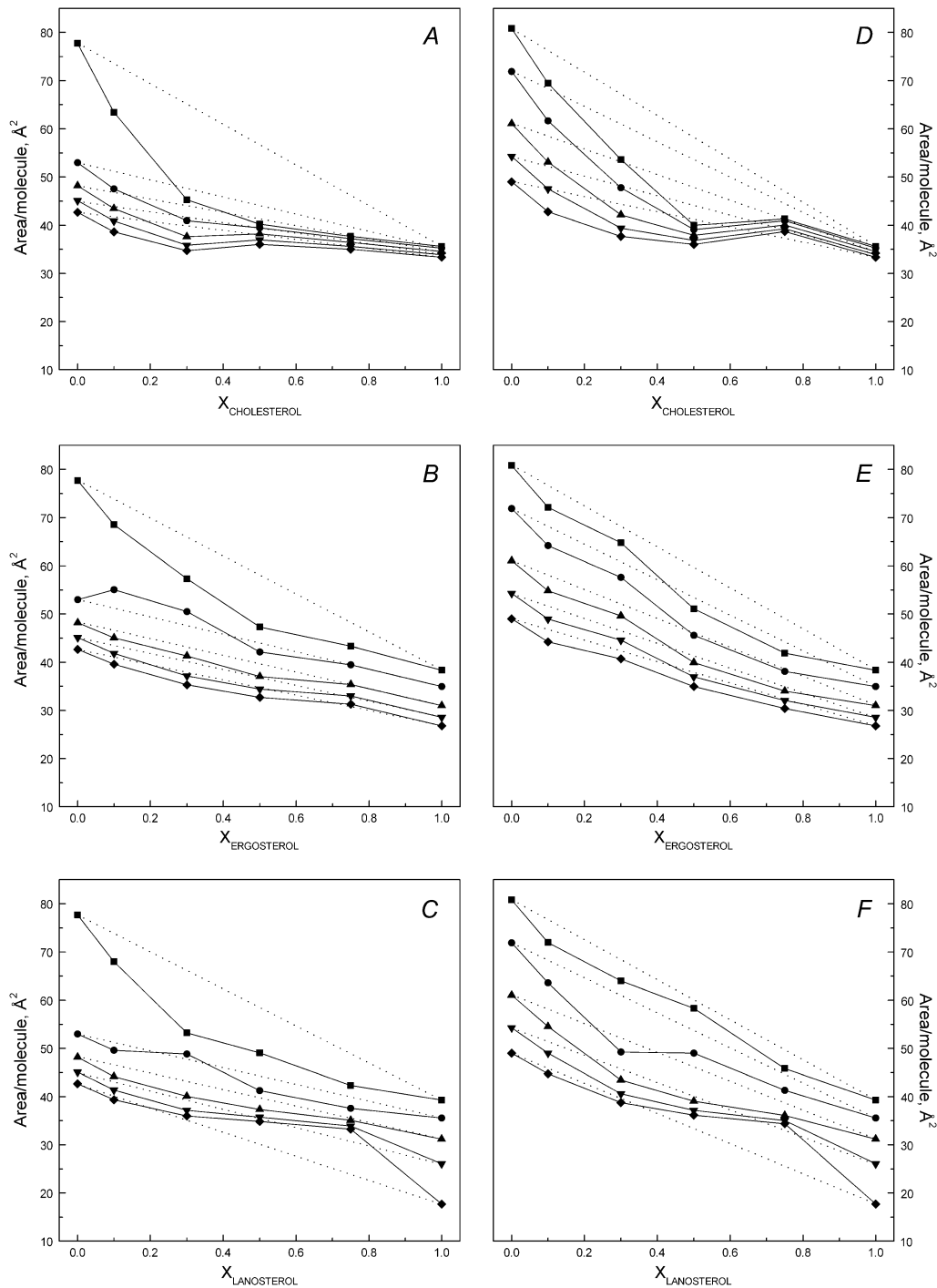


FIGURE 3 Variations in mean molecular areas \bar{A} vs. X_{sterol} for cholesterol (A and D), ergosterol (B and E), and lanosterol (C and F), respectively, as binary mixtures with DPPC (left) and DMPC (right) at 5 (■), 10 (●), 20 (▲), 30 (▼), and 40 (◆) mN/m are shown. The data were taken from the graphs in Fig. 2. The dotted lines represent the ideal miscibility behavior of the monolayer components.

The C_s^{-1} vs. π data (Fig. 4, A–C) for pure DPPC and mixed monolayers with $X_{\text{sterol}} = 0.1$ are similar, and the maximum value of C_s^{-1} reached in all cases is ~ 200 mN/m. The LE-LC transition is clearly visible in the above curves at a pressure between 5 and 10 mN/m. There are distinct differences in the impact of the three sterols. The transitions for pure DPPC and

$X_{\text{chol}} = 0.1$ overlap, whereas the transition is shifted for lanosterol and ergosterol at $X_{\text{sterol}} = 0.1$ to higher pressures in the sequence ergosterol > lanosterol > cholesterol. At $X_{\text{sterol}} = 0.3$ the LE-LC coexistence prevails for lanosterol at higher pressure (~ 12 mN/m), whereas it is not longer discernible for cholesterol and ergosterol. Yet, an inflection in these curves

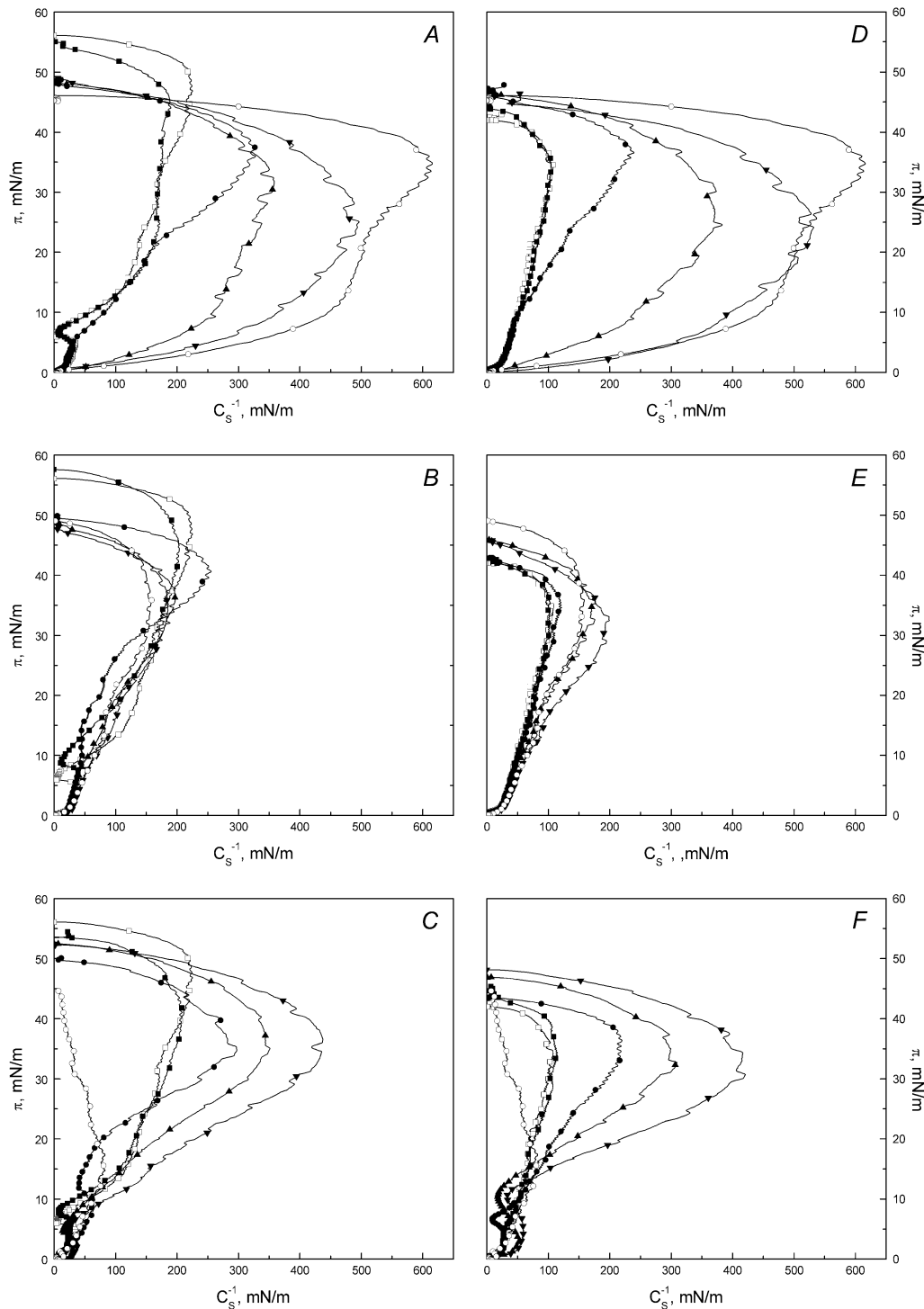


FIGURE 4 Values for π vs. C_s^{-1} calculated from the data in Fig. 2, for cholesterol (A and D), ergosterol (B and E), and lanosterol (C and F) in mixed monolayers with DPPC (left) and DMPC (right), with increasing X_{sterol} as 0.0 (\square), 0.1 (\blacksquare), 0.3 (\bullet), 0.5 (\blacktriangle), 0.75 (\blacktriangledown), and 1.0 (\circ).

between 10 and 20 mN/m can be seen. Whereas the values of C_s^{-1} for cholesterol and lanosterol increased proportionally to the increase of X_{sterol} , (with the exception for $X_{\text{chol}} = 0.1$ and pure lanosterol), a maximum is reached at $X_{\text{ergo}} = 0.3$ for ergosterol, with the C_s^{-1} values subsequently decreasing with increasing X_{sterol} .

The similarity of C_s^{-1} vs. π data for pure DMPC and mixed monolayers with $X_{\text{sterol}} = 0.1$ is even clearer than for DPPC. In this case, the curves are nearly identical, and the highest value of C_s^{-1} reached is ~ 100 mN/m. As expected, no discontinuities are detected. The data at $X_{\text{sterol}} = 0.3$ are similar for lanosterol and cholesterol, whereas the values for ergosterol

are close to those of pure DMPC. For lanosterol at X_{lamo} from 0.3 to 0.75, a pronounced transition at surface pressures between 5 and 12 mN/m is evident. For all three sterols, the values of C_s^{-1} increased proportionally to the increase of X_{sterol} , with the exception for pure ergosterol and pure lanosterol.

C_s^{-1} vs. X_{sterol} data at surface pressures ranging from 5 to 40 mN/m were plotted to better demonstrate the changes in

film compressibility modulus with varying X_{sterol} (Fig. 5). At pressures of 5 mN/m and 10 mN/m, the impacts of all three sterols mixed with DPPC or DMPC are similar. In contrast, in the pressure range of 20 to 40 mN/m, the compressibility of binary monolayers of sterols and DPPC exceeds that of films with DMPC for a sterol mole fraction of $X = 0.3$.

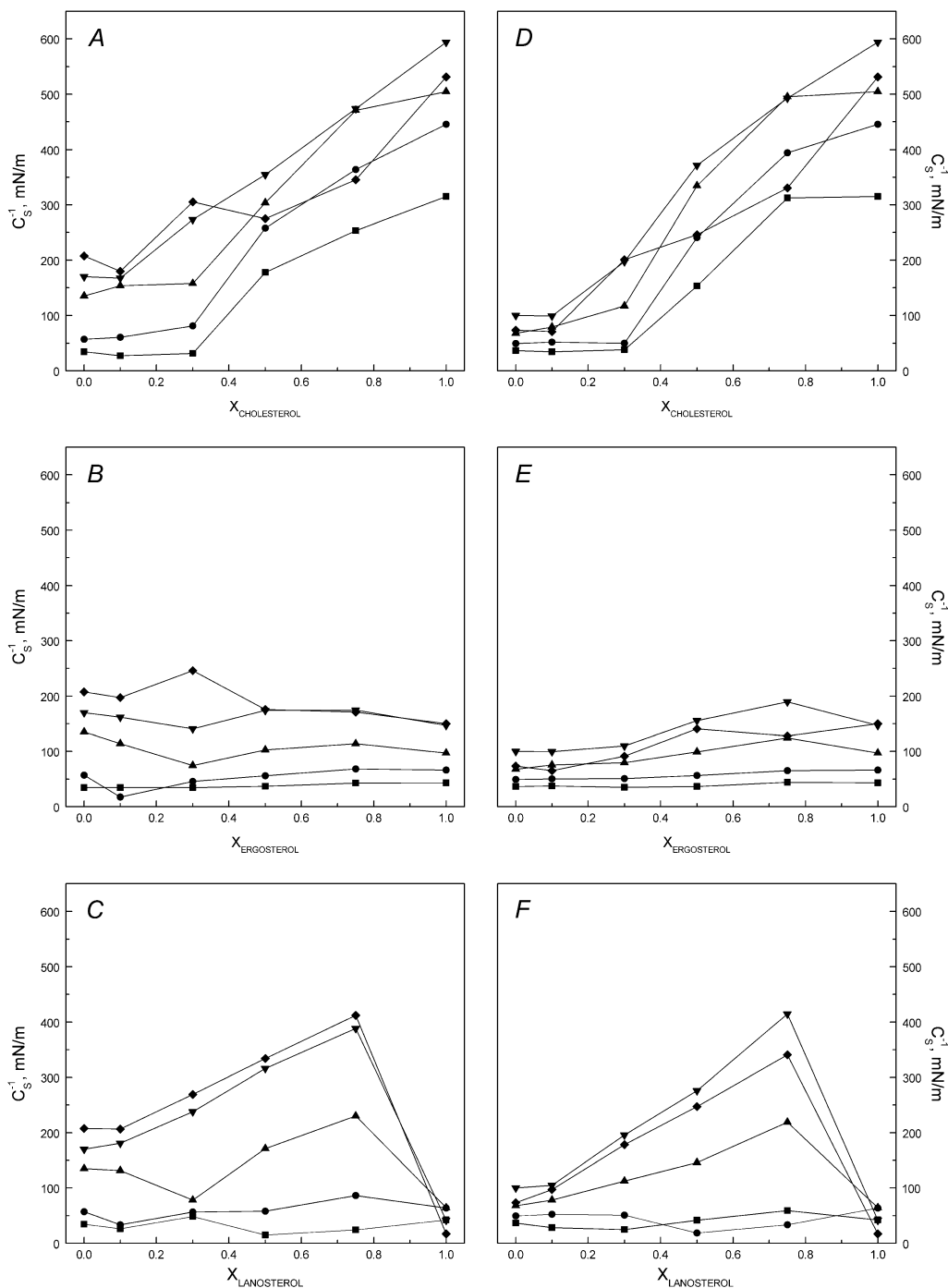


FIGURE 5 C_s^{-1} vs. X_{sterol} data at 5 (■), 10 (●), 20 (▲), 30 (▼), and 40 (◆) mN/m, are shown for cholesterol (A and D), ergosterol (B and E), and lanosterol (C and F) in DPPC (left) and DMPC (right) mixed monolayers. The data were taken from the graphs illustrated in Fig. 2.

$\Delta\psi$ - A isotherms

As for the π - A isotherm, pure DPPC reveals the typical LE-LC coexistence region with well-defined limits. Increasing X_{sterol} in DPPC decreases the range of millivolts for each surface potential isotherm (Fig. 6, A–C). For films containing cholesterol and ergosterol with $X_{\text{sterol}} = 0.1$, the main tran-

sition occurs at higher values of surface potential compared to pure DPPC, and there is significant overlap between the isotherms in the case of cholesterol. For binary mixtures with $X_{\text{lano}} = 0.1$, however, the whole isotherm is shifted to lower potentials. Films with X_{sterol} from 0.3 to 0.75 do not display the coexistence region. As a general trend, a decrease in

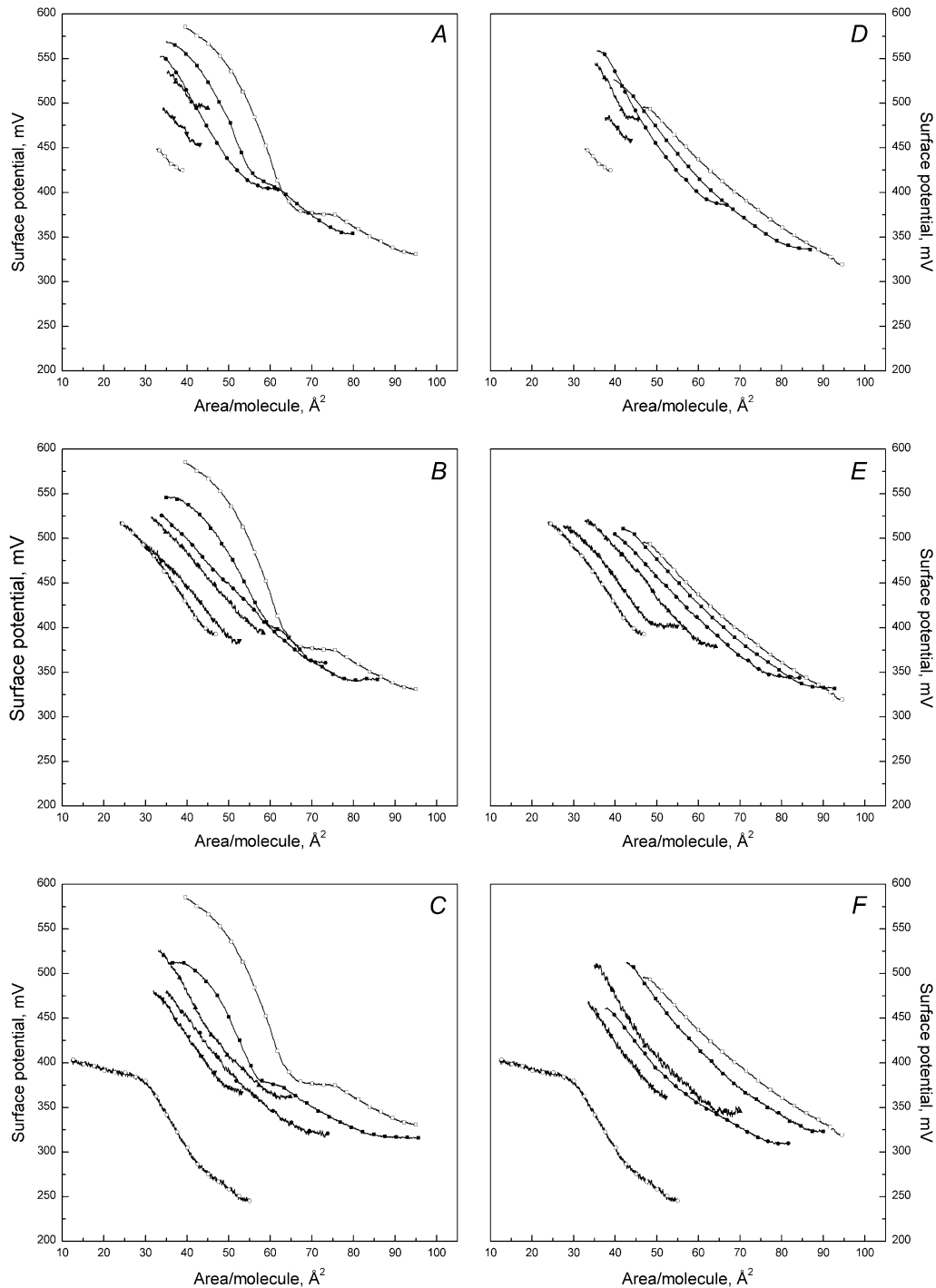


FIGURE 6 Representative surface potential $\Delta\psi$ vs. \bar{A} for cholesterol, ergosterol, and lanosterol in DPPC (A, B, and C, respectively), and in DMPC (D, E, and F, respectively) monolayers. X_{sterol} increases as 0.0 (\square), 0.1 (\blacksquare), 0.3 (\bullet), 0.5 (\blacktriangle), 0.75 (\blacktriangledown), and 1.0 (\circ).

surface potential is seen with increasing X_{sterol} . For $X_{\text{Iano}} = 0.5$, however, the isotherm is shifted toward higher potentials compared to $X_{\text{Iano}} = 0.3$; hence, it does not follow the behavior described above.

The surface potential isotherms of pure DMPC and with $X_{\text{sterol}} = 0.1$ (Fig. 6, *D–F*) are linear and nearly identical. At $X_{\text{sterol}} = 0.3$, cholesterol reveals higher surface potential than the isotherms for $X_{\text{sterol}} = 0.1$ and pure DMPC; for lanosterol, however, the potential is lower for higher mole fractions. As for DPPC, in binary mixtures with DMPC, the surface potential isotherm with $X_{\text{Iano}} = 0.5$ is shifted to higher potentials compared to $X_{\text{Iano}} = 0.3$. Further, no pronounced transition is evident, contrary to what is expected on the basis of the π - A isotherm. However, the $\Delta\psi$ - A data for $X_{\text{Iano}} = 0.3$ display three different slopes, of which the middle one (at ~ 50 – 60 \AA^2) coincides with the shoulder evident in the π - A isotherm. For pure lanosterol, the surface potential curve bends at an area/molecule value of ~ 31 – 32 \AA^2 , that is, at the same point in which the compression isotherm bends and continues toward higher value of pressure following the new slope.

To better illustrate the difference between the three sterols in the two host matrices, we plotted $\Delta\psi$ vs. X_{sterol} isobars at 5, 10, 20, 30, and 40 mN/m (Fig. 7). For DMPC, all isobars for the sterols follow the same trend with the surface potential values with $X_{\text{sterol}} = 0.1$ exceeding those for pure DMPC. Instead, for $X_{\text{sterol}} = 0.3$, cholesterol has higher surface potential than that of $X_{\text{sterol}} = 0.1$, whereas there are only minor differences for different contents of ergosterol. For films containing lanosterol ψ reaches a minimum at $X_{\text{Iano}} = 0.3$. For mixtures of the sterols and DPPC, the isobars at 5 mN/m are always different from the trend observed for higher surface pressures.

Values for the monolayer dipole moment vector perpendicular to the monolayer plane (μ_{\perp}) were calculated by fitting Eq. 3 to $\Delta\psi$ vs. $1/A$ data and then plotted against area/molecule (Fig. 8). The data for pure phospholipids reveal two different slopes for DMPC, whereas DPPC presents a plateau corresponding to the LE region in the compression isotherm, a minimum corresponding to the center of the LE-LC coexistence region, and a maximum corresponding to the onset of the LC region. Moreover, it is of interest to note that the beginning and the end of the LE-LC region are represented by two lines with negative and positive slopes, respectively. In mixed monolayers of DPPC with $X_{\text{sterol}} = 0.1$, the trend seen for pure DPPC is present (with a plateau, a minimum, and a maximum); however, all three curves start to increase at lower values of area/molecule. Starting from $X_{\text{sterol}} = 0.3$, this trend is no longer seen and only minor differences are evident in the μ_{\perp} vs. A data between monolayers of pure DMPC and those with X_{sterol} between 0.1 and 0.75. Of particular interest are films with X_{Iano} ranging from 0.3 to 0.75 because these compositions present a pronounced transition in the π - A isotherms. Accordingly, careful inspection of the μ_{\perp} vs. A data reveals a slight inflection at ~ 55 – 60 \AA^2 , ~ 50 – 55 \AA^2 , and ~ 40 – 45 \AA^2 for $X_{\text{Iano}} = 0.3$, 0.5, and 0.75, respectively.

The excess free energy of mixing ($\Delta G_{\text{mix}}^{\text{exc}}$)

To investigate the thermodynamic stability of the mixed monolayers compared to the monolayers of the pure components, we constructed $\Delta G_{\text{mix}}^{\text{exc}}$ vs. π curves (Fig. 9). In brief, negative values of $\Delta G_{\text{mix}}^{\text{exc}}$ indicate that mixing of the monolayer constituents is favored because of attractive intermolecular interactions. In contrast, positive values of $\Delta G_{\text{mix}}^{\text{exc}}$ suggest thermodynamic instability of the mixed monolayers (28,29).

Analysis of the $\Delta G_{\text{mix}}^{\text{exc}}$ vs. π for mixed sterol/DPPC films reveals an initial decrement in $\Delta G_{\text{mix}}^{\text{exc}}$ for all mole fractions of the three sterols. Subsequently, at higher surface pressures, binary mixtures containing cholesterol continue to give negative values of $\Delta G_{\text{mix}}^{\text{exc}}$. Notably, $\Delta G_{\text{mix}}^{\text{exc}}$ decreases in a progressive manner in the sequence $X_{\text{chol}} = 0.3 < X_{\text{chol}} = 0.5 < X_{\text{chol}} = 0.1 < X_{\text{chol}} = 0.75$. After an initial decrement, mixed monolayers containing ergosterol at $X = 0.1$ and 0.3 display local maxima in $\Delta G_{\text{mix}}^{\text{exc}}$ at $\pi \approx 15$ mN/m. For $X_{\text{ergo}} = 0.5$, after a sharp initial decrement, $\Delta G_{\text{mix}}^{\text{exc}}$ continues to decrease linearly toward more negative values, whereas the opposite behavior is evident for $X_{\text{ergo}} = 0.75$, with the free energy becoming less negative with increasing π . Data for $X_{\text{Iano}} = 0.1$ contain, after an initial decrement, a local maximum at $\pi \approx 10$ mN/m, whereas this maximum is shifted to $\pi \approx 15$ mN/m for $X_{\text{Iano}} = 0.3$. Films with $X_{\text{Iano}} = 0.5$ and 0.75 present negative values until the pressure of 30 and 20 mN/m, respectively. Starting from this pressure, the $\Delta G_{\text{mix}}^{\text{exc}}$ values for $X_{\text{Iano}} = 0.75$ rise toward zero, and, at a pressure of ~ 40 mN/m, they become slightly positive.

In mixed monolayers with DMPC, all three sterols at $X_{\text{sterol}} = 0.1$ reveal negative values of $\Delta G_{\text{mix}}^{\text{exc}}$ decreasing nearly linearly with increasing surface pressure. The two curves with the most interesting behavior are 1), $X_{\text{Iano}} = 0.75$, which first decreases and, starting from a pressure of ~ 25 mN/m, constantly moves toward less negative values of $\Delta G_{\text{mix}}^{\text{exc}}$ with increasing surface pressure; and 2), $X_{\text{Iano}} = 0.5$, which exhibits a shoulder in the pressure range of 5 to 15 mN/m. Subsequently, the values of $\Delta G_{\text{mix}}^{\text{exc}}$ for this composition decrease, reaching a minimum at ~ 35 mN/m. Upon further increase in surface pressure, $\Delta G_{\text{mix}}^{\text{exc}}$ starts to increase again.

DISCUSSION

The presence of sterols causes the phospholipid acyl chains close to the headgroup to have predominantly a *trans* configuration, leading to an increase in bilayer thickness (32). Results of small-angle neutron scattering studies (9) indicate an increase in the thickness of DMPC bilayers due to the presence of all three sterols used in this study. These results can be interpreted as a consequence of the ordering effect imposed by the sterol molecules sandwiched between phospholipid acyl chains. Membrane hydrophobic thickness is known to be an important determinant of lipid bilayer and integral protein interactions, in particular regarding the in-

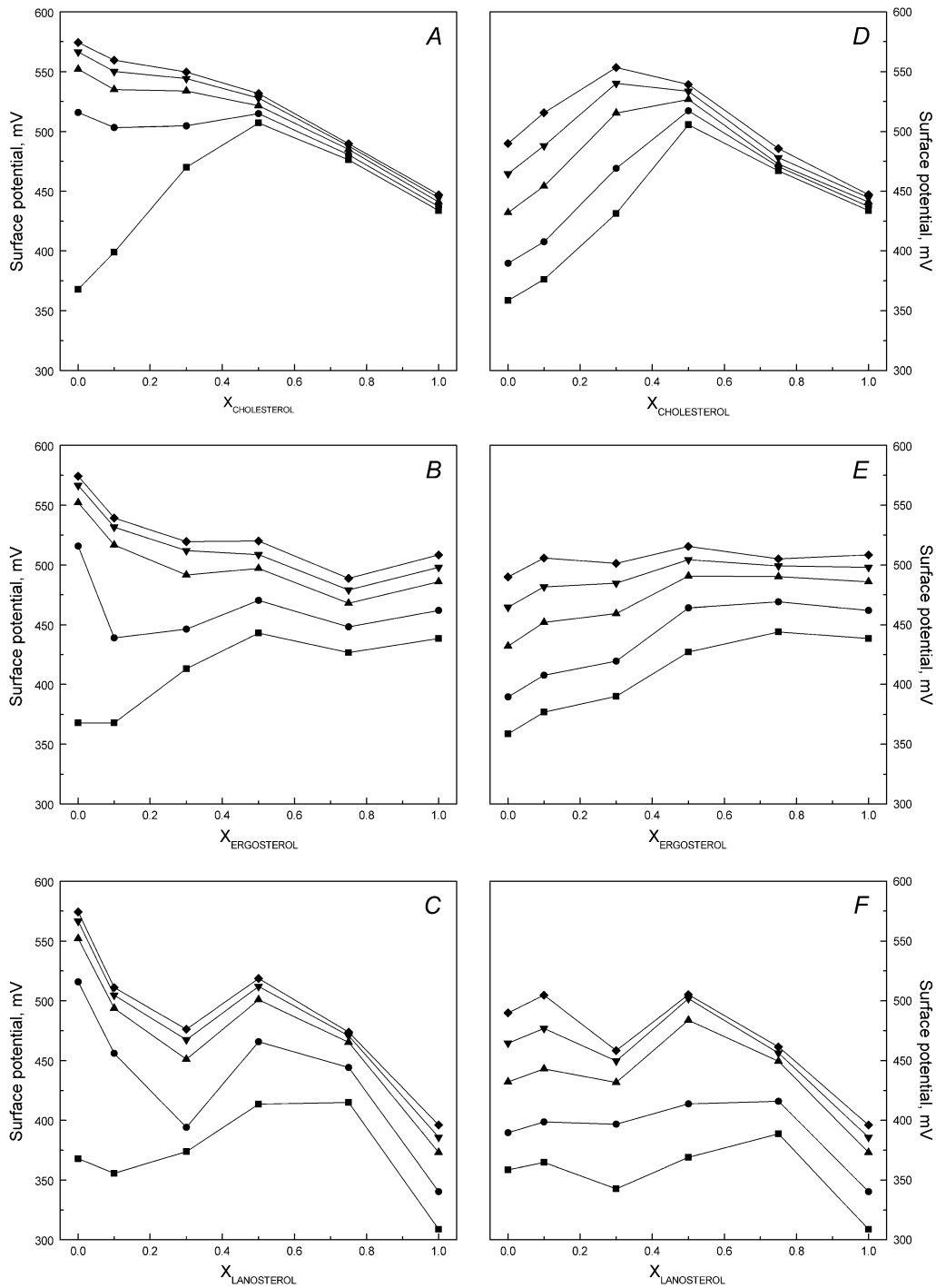


FIGURE 7 Isobars for $\Delta\psi$ vs. X_{sterol} data for cholesterol (A and D), ergosterol (B and E), and lanosterol (C and F), respectively, in binary mixtures with DPPC (left) and DMPC (right), at constant lateral pressure of 5 (■), 10 (●), 20 (▲), 30 (▼), and 40 (◆) mN/m are shown.

sertion, folding, assembly and function of transmembrane proteins (9,18). As a consequence of the change in thickness, there are also modifications in membrane permeability, the latter being a decreasing function of the bilayer thickness (33). It is further known that sterols (in particular, cholesterol and ergosterol) are distributed nonrandomly in domains, which are further implicated in cell signaling and traffic, with

their membrane content under stringent control (3,34). The importance of sterols and, in particular, cholesterol in these domains is demonstrated by the fact that even if the formation of domains persist after the replacement of cholesterol with its close precursor 7-dehydrocholesterol, a clear difference in their protein composition is caused, thereby provoking modifications of membrane properties and cellular physiology

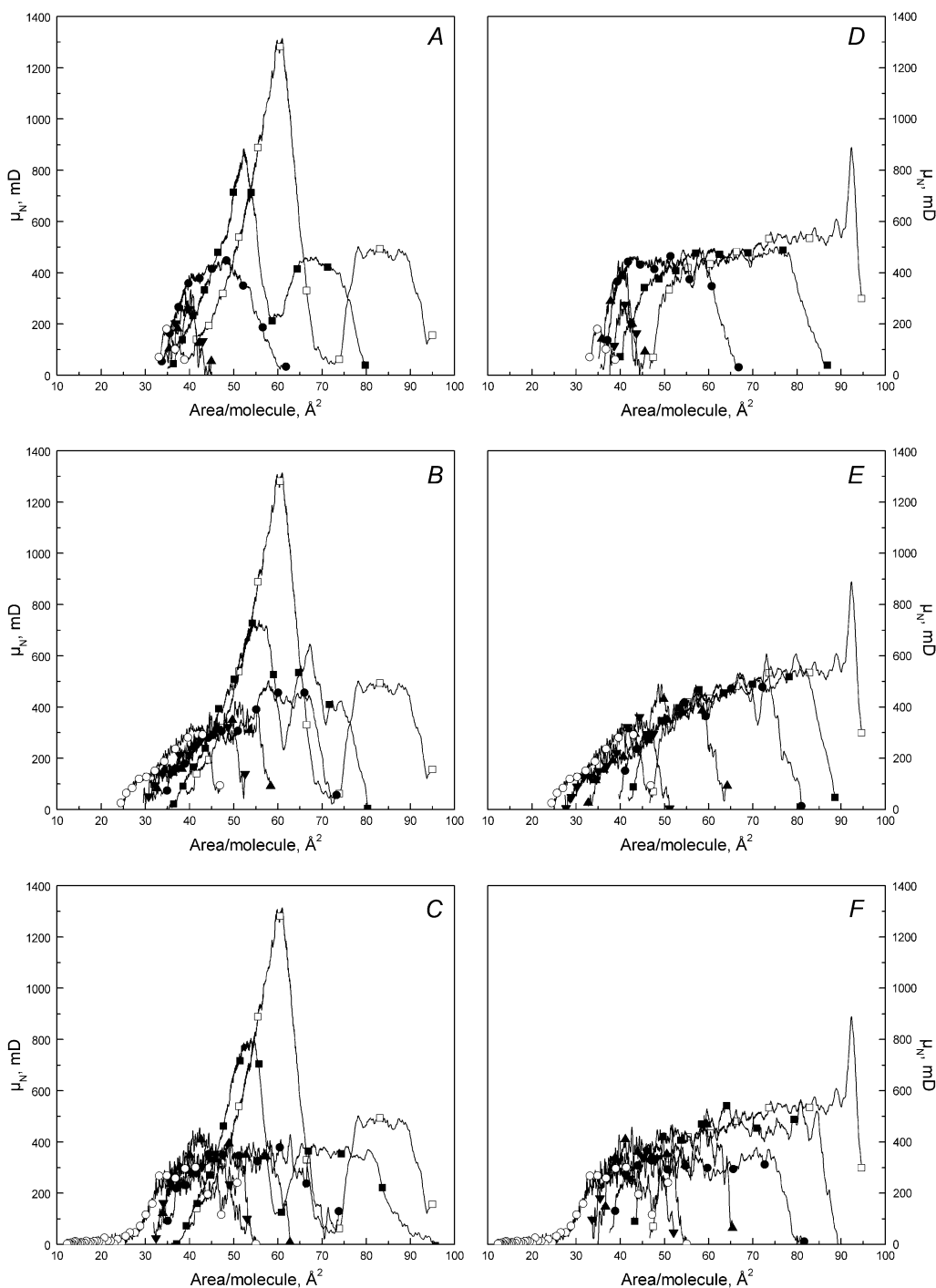


FIGURE 8 μ_{\perp} vs. X_{sterol} for cholesterol (A and D), ergosterol (B and E), and lanosterol (C and F), in binary mixtures with DPPC (left) and DMPC (right), containing films with increasing X_{sterol} as 0.0 (\square), 0.1 (\blacksquare), 0.3 (\bullet), 0.5 (\blacktriangle), 0.75 (\blacktriangledown), and 1.0 (\circ).

(34,35). Moreover, it has been demonstrated that cholesterol has a major impact on the lateral pressure profile of a bilayer and may thus regulate membrane protein functions (36). Cholesterol also confers negative spontaneous curvature to the lipid bilayer (37–39), thus facilitating membrane fusion (40,41). Because of the above features and because of the presence of sterols in different kingdoms, it was of interest to

compare the surface properties of cholesterol, ergosterol, and lanosterol despite few and small differences in their structures.

The presence of sterols in mixed monolayers with DPPC or DMPC imparts pronounced effects on the compression isotherms. As reported previously (12,42,43), increasing the content of cholesterol in a DPPC monolayer causes a pro-

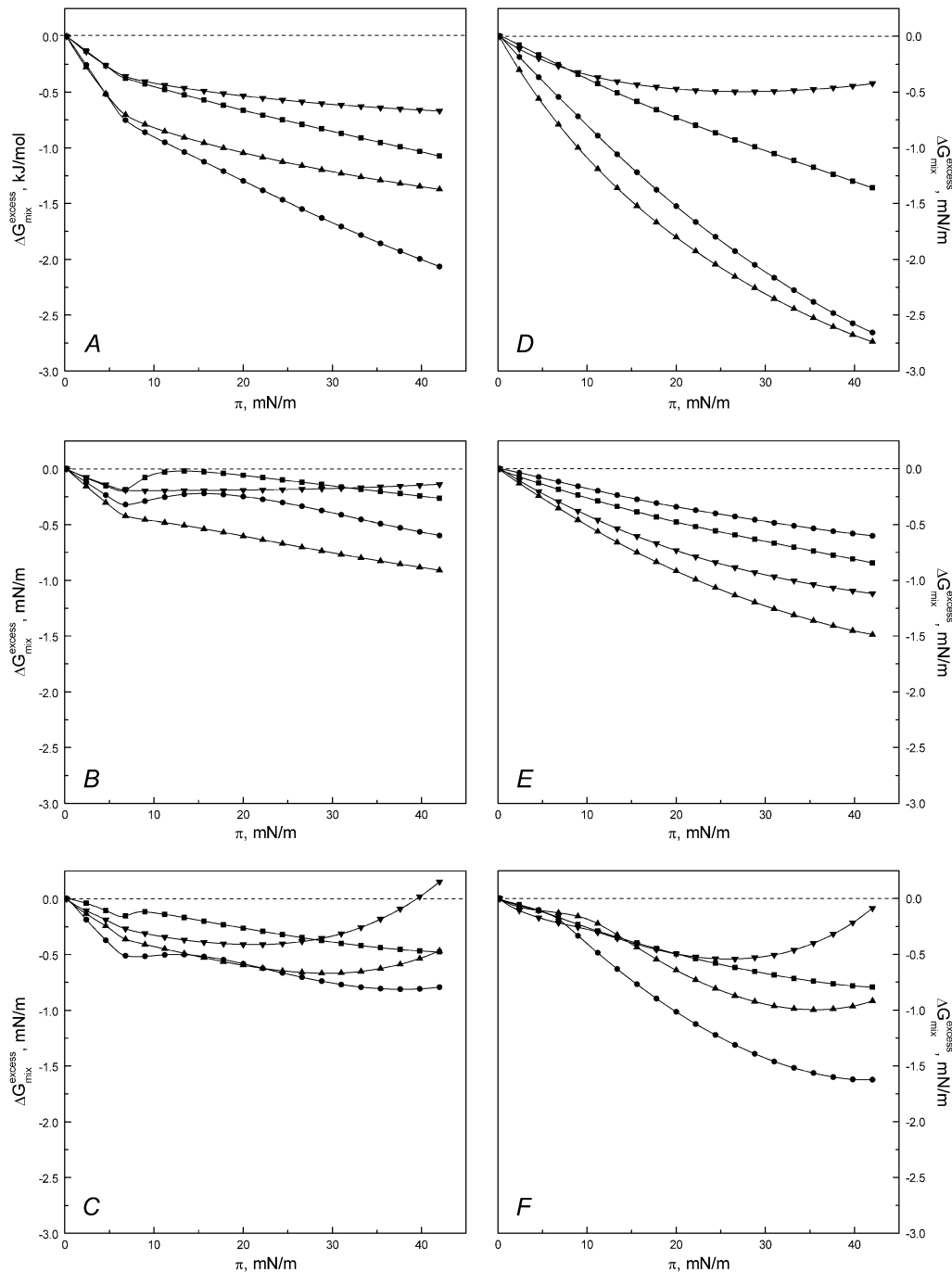


FIGURE 9 Variation in the excess free energy of mixing $\Delta G_{\text{mix}}^{\text{excess}}$ vs. π_s for cholesterol (A and D), ergosterol (B and E), and lanosterol (C and F), in binary mixtures with DPPC (left) and DMPC (right), with increasing X_{sterol} as (■) 0.1, and (●) 0.3, (▲) 0.5, and (▼) 0.75. The data were taken from the graphs in Fig. 2.

gressive disappearance of the LE-LC coexistence region and shifts the isotherms to the left (i.e., to lower values of area/molecule), evident as the “condensing effect” of cholesterol in phospholipid monolayers (29,32,34,42). In other words, the interaction between cholesterol and phospholipids, with hydrogen bonding and van der Waals attraction acting as stabilizing forces, increases the structural order of the phospholipid hydrocarbon acyl chains and so results in an in-

crease in the packing density of the monolayer. This condensation also results from the partial accommodation of cholesterol underneath the hydrated phosphocholine head-group, referred to as the “umbrella effect” (44,45). This behavior is due to the necessity for cholesterol to have a larger hydration shell than its own to avoid (energetically unfavorable) contacts of its hydrophobic parts with water (46,47). In the light of this study, it is evident that not only

cholesterol but also lanosterol and ergosterol induce condensation in mixed monolayers with DPPC and DMPC.

To obtain further insight into the condensing effect seen in compression isotherms, we proceeded to analyze the mean molecular area \bar{A} vs. X_{sterol} data. Cholesterol exerts a pronounced condensing effect in DPPC monolayers, in particular at low surface pressures (i.e., 5 mN/m), and this prevails for the whole range of analyzed pressures and all mole fractions in the mixed films. Condensation due to ergosterol and lanosterol is most significant at low pressures, albeit less pronounced compared to cholesterol. Data for ergosterol reveal an expansion at $\pi \sim 10$ mN/m at $X_{\text{ergo}} < 0.5$ and a slight condensation for all the other pressures and monolayer compositions. Lanosterol, however, produces a pronounced film expansion at high surface pressures when present at high mole fractions. The above behavior can be attributed to the differences in the structures of the sterols. The methyl group and the double bond present in the alkyl chain of ergosterol could be responsible for the expansion. Yet, this could be counterbalanced by the presence of the second double bond in the rigid ring, because the latter can increase the conformational order of the lipid acyl chains (4), leading to an enhanced van der Waals attraction and thus augmented lateral packing, especially at higher surface pressures. Another possibility to explain the expansion due to ergosterol could be a slightly different position of the molecule itself with respect to the DPPC bilayer (13). Instead, due to lanosterol, the increased expansion at higher packing densities would comply with steric crowding because of the three methyl groups. The condensing effect vanishes in the presence of additional methyl groups in the ring system (4), and so lanosterol, with its bulkier sterol body, can be expected to be less effective than the other sterols in causing monolayer condensation (4,13). Because it is easier to accommodate additional chemical groups into a liquid expanded matrix at higher surface pressures in particular, it was not surprising to find a more pronounced condensation for DMPC and less pronounced expansion for all three sterols in the pressure range studied. The behavior of lanosterol at low pressures might result from a stronger interaction between the hydrophobic regions of these sterols and the acyl chains of DMPC, which are two carbons shorter than for DPPC.

For monomolecular lipid films, it is possible to analyze with high precision the differences in physical state due to the sterols by observing the maximum compressibility modulus (29,31). According to Davies and Rideal (48), C_s^{-1} values in the range of 100 to 250 mN/m are indicative of the liquid-condensed state, whereas values above 250 mN/m reveal the presence of the solid state, characterized by close packing of the hydrocarbon chains in the monolayer. Thus, from the analysis of our data (Figs. 4 and 5, and Table 1), it appears that films with $X_{\text{sterol}} = 0.3$ in the DPPC matrix are in a solid phase with values of C_s^{-1} increasing in the order ergosterol < lanosterol < cholesterol, with the value for ergosterol being close to the LC region. Interestingly, all the other composi-

TABLE 1 Maximum compressibility moduli (C_s^{-1}) and the corresponding surface pressures (π_{max}) measured for the binary phospholipid/sterol monolayers

		C_s^{-1} (mN/m)		π_{max} (mN/m)	
		DPPC		DMPC	
X_{sterol}	0.0	223.8	47.7	107.5	34.2
X_{chol}	0.1	188.3	44.0	106.9	34.6
	0.3	326.8	38.2	237.6	36.6
	0.5	357.6	32.4	377.1	26.5
	0.75	494.7	25.1	529.3	24.1
	1.0	615.0	34.8	615.0	34.8
X_{ergo}	0.1	203.4	44.4	102.8	35.5
	0.3	253.6	40.8	120.1	34.5
	0.5	197.8	36.4	171.9	34.0
	0.75	184.5	35.4	194.7	32.4
	1.0	157.0	35.2	157.0	35.2
X_{lano}	0.1	208.9	38.9	113.8	34.3
	0.3	284.7	35.6	220.5	34.6
	0.5	346.7	36.6	306.2	34.5
	0.75	436.9	35.8	419.0	32.3
	1.0	80.6	13.7	80.6	13.7

tions analyzed for ergosterol show that these films remain in the LC phase. Also in DMPC, all compositions analyzed for ergosterol display values in the range indicative of the LC phase, whereas for cholesterol and lanosterol, films with $X_{\text{sterol}} \geq 0.5$ enter the solid phase upon compression.

The disappearance of the LE-LC coexistence region due to high contents of cholesterol does not necessarily mean that the system becomes more “solid-like” (10,12). Cholesterol, because of its rigid structure, interacts with phospholipids in two different ways: it induces chain ordering and, at the same time, it interacts with the lateral packing order of the solid phase (s_o), tending to break it. The result is the formation of a new phase called the liquid-ordered state (l_o), in which the molecules behave as in a fluid with respect to mobility and orientation, but they possess a high degree of orientational order of the acyl chains similar to the condensed state (49). The phase diagram of fully hydrated PC/cholesterol bilayers for all temperatures shows the presence of the l_o state alone for $X_{\text{chol}} \geq 0.25$ –0.30, and the presence of $l_o + s_o$ for X_{chol} between 0.10 and 0.30 (10,12). Mixtures of DPPC and cholesterol present a single uniform liquid phase at temperatures above the DPPC chain melting temperature of 41°C (50). Ergosterol also promotes the formation of the l_o state, albeit less effectively than cholesterol and necessitating a higher content of this sterol compared to cholesterol (51). Larger mole fractions of lanosterol have been found to yield the l_o state but always in association with the liquid-disordered (l_d) state. Also, in a range of $X_{\text{lano}} = 0.10$ –0.30, it is possible to find coexisting $s_o + l_d/l_o$ states (10,52).

The phase diagrams of the mixtures of the three sterols with phospholipids have been constructed on the basis of data from experiments using lamellar systems. It is important to note that the correlation between the content of sterols that

can provoke a state modification in bilayers and monolayers, respectively, has not been thoroughly established. Using fluorescence microscopy, Stottrup and Keller (6) observed distinct α - and β -regions (at low and high sterol content, respectively) of liquid-liquid coexistence in binary DPPC/sterol monolayers, possibly arising from formation of condensed DPPC/sterol complexes and subsequent demixing between the complexes and the bulk monolayer (53). Evaluating our data in this context, there is a sudden increase in the compressibility modulus of DPPC/cholesterol monolayers going from $X_{\text{chol}} = 0.3$ to 0.5 (Fig. 5 A), that is, entering the β -region. However, a similar increase is not evident for ergosterol-containing monolayers (Fig. 5 B), also displaying a β -region boundary between $X_{\text{ergo}} = 0.3$ and 0.5 (6); the values for C_5^{-1} remain essentially constant for all the values of X_{ergo} studied. The surface potential values of DPPC/cholesterol monolayers recorded at different surface pressure values converge at $X_{\text{chol}} = 0.5$ (Fig. 7 A). Below this mole fraction, the potential values at 5 mN/m are considerably lower, possibly reflecting the presence of the α -region of immiscibility observed for low sterol content and low packing densities (21). Somewhat analogously, albeit less pronounced behavior is observed for ergosterol. The behavior of lanosterol, which according to Stottrup and Keller (6) does not induce liquid-liquid coexistence in mixed monolayers with DPPC, does not differ dramatically from the two other sterols with respect to modulation of monolayer compressibility or surface potential. This further suggests that the correlation of phase separation and these two monolayer bulk physical properties cannot be unambiguously resolved. In addition, Stottrup and Keller (6) failed to form stable monolayers of neat lanosterol. This discrepancy might be related to enhanced hydrophobicity due to the 15 mM NaCl included in the subphase in our experiments, resulting in increased stability of the monolayers.

Although a considerable fraction of the monolayer components can be oriented parallel to the subphase surface for high values of area/molecule, this is unlikely at higher packing densities. Moreover, it has been shown that, in a bilayer, lanosterol and ergosterol remain confined to their monolayer, whereas cholesterol can move in the transverse direction over a longer distance (1 nm) (14). In a dipolyunsaturated PC bilayer, the hydroxyl end of the cholesterol may relocate to the center of the bilayer in an upside-down orientation, as well as perpendicularly to the bilayer normal at the interface between the two monolayers (54). Moreover, cholesterol and ergosterol decrease bilayer hydration because condensation reduces water penetration into membrane (55,56). These features can explain the reduction of the potential gap and the shifting of the main phase transition toward higher potential values in our data (Fig. 6), the latter effect being more pronounced for cholesterol. For lanosterol, there is a reduction of the potential gap and, increasing X_{lano} , the curves are shifted toward lower values (Fig. 6). There is no evidence in the compression isotherms for relocation of

lanosterol toward the headgroup region or the subphase. Moreover Endress et al. (14) pointed out that these kind of movements are unlikely due to the energy balance. Lanosterol does not induce condensation as efficiently as cholesterol, and it is less effective in reducing membrane permeability (32). Accordingly, the decrease in ψ could be explained by an increase in the number of water molecules in the membrane. Notably, the ability to modify acyl chain order, condensation, and permeability are inversely proportional to the tilt of cholesterol in the membrane (57), and recent molecular dynamics studies suggest the tilt angle to increase upon introduction of double bonds in the sterols' tail structures, zero for cholesterol and one for ergosterol and lanosterol, in positions C_{22} and C_{24} , respectively (58,59). A larger tilt angle can also explain why a higher surface pressure at $X_{\text{sterol}} = 0.1$ is needed to induce the LE-LC coexistence in DPPC monolayers containing ergosterol or lanosterol compared to cholesterol (Fig. 1, A–C).

Finally, irrespective of the host matrix (DMPC or DPPC), the values of the excess free energy of mixing show that most stable monolayers are those containing cholesterol (in particular DPPC with $X_{\text{chol}} = 0.3$ and DMPC with $X_{\text{chol}} = 0.5$), especially at surface pressure values prevailing in natural membranes, estimated to vary from ~ 30 to ~ 35 mN/m (60). Accordingly, it is tempting to speculate that this property of cholesterol provides the appropriate environment for more complex membrane systems and allows for improved adjustment of the membrane hydrophobic thickness required for the proper functioning of more sophisticated protein assemblies.

The authors thank Kristiina Söderholm for skillful technical assistance.

H.B.B.G. was supported by the Finnish Academy, the Marie Curie Training Network, and the Sigrid Jusélius Foundation.

REFERENCES

- Bloch, K. 1983. Sterol structure and membrane function. *CRC Crit. Rev. Biochem.* 14:47–92.
- Urbina, J. A., S. Pekerar, H. B. Le, J. Patterson, B. Montez, and E. Oldfield. 1995. Molecular order and dynamics of phosphatidylcholine bilayer membranes in the presence of cholesterol, ergosterol and lanosterol: a comparative study using ^2H -, ^{13}C - and ^{31}P -NMR spectroscopy. *Biochim. Biophys. Acta.* 1238:163–176.
- Arora, A., H. Raghuraman, and A. Chattopadhyay. 2004. Influence of cholesterol and ergosterol on membrane dynamics: a fluorescent approach. *Biochem. Biophys. Res. Commun.* 318:920–926.
- Bernsdorff, C., and R. Winter. 2003. Differential properties of the sterols cholesterol, ergosterol, β -sitosterol, *trans*-7-dehydrocholesterol, stigmasterol and lanosterol on DPPC bilayer order. *J. Phys. Chem. B.* 107:10658–10664.
- Nes, W. R. 1974. Role of sterols in membranes. *Lipids.* 9:596–612.
- Stottrup, B. L., and S. Keller. 2006. Phase behavior of lipid monolayers containing DPPC and cholesterol analogs. *Biophys. J.* 90:3176–3183.
- Henriksen, J., A. C. Rowat, E. Brief, Y. W. Hsueh, J. L. Thewalt, M. J. Zuckermann, and J. H. Ipsen. 2006. Universal behavior of membranes with sterols. *Biophys. J.* 90:1639–1649.
- Bloch, K. 1985. Cholesterol, evolution of structure and function. Benjamin/Cummings, New York.

9. Pencer, J., M. P. Nieh, T. A. Harroun, S. Krueger, C. Adams, and J. Katsaras. 2005. Bilayer thickness and thermal response of dimyristoylphosphatidylcholine unilamellar vesicle containing cholesterol, ergosterol and lanosterol: a small-angle neutron scattering study. *Biochim. Biophys. Acta.* 1720:84–91.
10. Miao, L., M. Nielsen, J. Thewalt, J. H. Ipsen, M. Bloom, M. J. Zuckermann, and O. G. Mouritsen. 2002. From lanosterol to cholesterol: structural evolution and differential effects on lipid bilayers. *Biophys. J.* 82:1429–1444.
11. Henriksen, J., A. C. Rowat, and J. H. Ipsen. 2004. Vesicle fluctuation analysis of the effects of sterols on membrane bending rigidity. *Eur. Biophys. J.* 33:732–741.
12. Bloom, M., and O. G. Mouritsen. 1995. The evolution of membranes. In *Handbook of Biological Physics*, Vol. 1. R. Lipowsky, and E. Sackmann, editors. Elsevier Science, Amsterdam. 65–95.
13. Endress, E., S. Bayerl, K. Prechtel, C. Maier, R. Merkel, and T. M. Bayerl. 2002. The effect of cholesterol, lanosterol and ergosterol on lecithin bilayer; mechanical properties at molecular and microscopic dimensions: a solid-state NMR and micropipette study. *Langmuir.* 18:3293–3299.
14. Endress, E., H. Heller, H. Casalta, M. F. Brown, and T. M. Bayerl. 2002. Anisotropic motion and molecular dynamics of cholesterol, lanosterol and ergosterol in lecithin bilayers studied by quasi-elastic neutron scattering. *Biochemistry.* 41:13078–13086.
15. Bloch, K. 1965. The biological synthesis of cholesterol. *Science.* 150:19–28.
16. Dahl, C., J. Dahl, and K. Bloch. 1980. Effect of alkyl-substituted precursor of cholesterol on artificial and natural membranes and on the viability of *Mycoplasma capricolum*. *Biochemistry.* 19:1462–1467.
17. Xu, X., R. Bittman, G. Duportail, D. Heissler, C. Vilcheze, and E. London. 2001. Effect of the structure of natural sterols and sphingolipids on the formation of ordered sphingolipid/sterol domains (rafts). *J. Biol. Chem.* 276:33540–33546.
18. Ipsen, J. H., O. G. Mouritsen, and M. Bloom. 1990. Relationship between lipid membrane area, hydrophobic thickness, and acyl-chain orientational order. *Biophys. J.* 57:405–412.
19. Bloom, M., and O. G. Mouritsen. 1988. The evolution of membranes. *Can. J. Chem.* 66:706–712.
20. Xu, X., and E. London. 2000. The effect of sterol structure on membrane lipid domains reveals how cholesterol can induce lipid domain formation. *Biochemistry.* 39:843–849.
21. Ali, M. D., K. H. Cheng, and J. Huang. 2007. Assess the nature of cholesterol-lipid interactions through the chemical potential of cholesterol in phosphatidylcholine bilayers. *Proc. Natl. Acad. Sci. USA.* 104:5372–5377.
22. Brockman, H. L. 1999. Lipid monolayers: why use half a membrane to characterize protein-membrane interaction? *Curr. Opin. Struct. Biol.* 9:438–443.
23. Brockman, H. L. 1994. Dipole potential of lipid membranes. *Chem. Phys. Lipids.* 73:57–79.
24. Benvegnu, D. J., and H. M. McConnell. 1993. Surface dipole densities in lipid monolayers. *J. Phys. Chem.* 97:6686–6691.
25. Coban, O., J. Popov, M. Burger, D. Vobornik, and L. J. Johnston. 2007. Transition from nanodomains to microdomains induced by exposure of lipid monolayers to air. *Biophys. J.* 92:2842–2853.
26. Brockman, H. L., C. M. Jones, C. J. Schwebke, J. M. Smaby, and D. E. Jarvis. 1980. Application of a microcomputer-controlled film balance system to collection and analysis of data from mixed monolayers. *J. Colloid Interface Sci.* 78:502–512.
27. Smaby, J. M., V. S. Kulkarni, M. Momsen, and R. E. Brown. 1996. The interfacial elastic packing interactions of galactosylceramides, sphingomyelins, and phosphatidylcholines. *Biophys. J.* 70:868–877.
28. Gong, K., S. S. Feng, M. L. Go, and P. H. Soew. 2002. Effects of pH on the stability and compressibility of DPPC/cholesterol monolayers at the air-water interface. *Colloid Surf. A—Physicochem. Eng. Asp.* 207:113–125.
29. Dynarowicz-Latka, P., and K. Hac-Wydro. 2004. Interactions between phosphatidylcholines and cholesterol in monolayers at the air/water interface. *Colloid Surf. B—Biointerfaces.* 37:21–25.
30. Phillips, M. C., and D. Chapman. 1968. Monolayer characteristics of saturated 1,2-diacyl phosphatidylcholines (lecithins) and phosphatidylethanolamines at the air-water interface. *Biochim. Biophys. Acta.* 163:301–313.
31. Kodama, M., O. Shibata, S. Nakamura, S. Lee, and G. Sugihara. 2004. A monolayer study on three binary mixed systems of dipalmitoyl phosphatidyl choline with cholesterol, cholestanol and stigmasterol. *Colloids Surf. B Biointerfaces.* 33:211–226.
32. Yeagle, P. L. 1985. Cholesterol and the cell membrane. *Biochim. Biophys. Acta.* 822:267–287.
33. Nezil, F. A., and M. Bloom. 1992. Combined influence of cholesterol and synthetic amphiphilic peptides upon bilayer thickness in model membranes. *Biophys. J.* 61:1176–1183.
34. Berring, E. E., K. Borrenpohl, S. J. Fliesler, and A. Barnoski Serfis. 2005. A comparison of the behavior of cholesterol and selected derivatives in mixed sterol-phospholipid Langmuir monolayers: a fluorescence microscopy study. *Chem. Phys. Lipids.* 136:1–12.
35. Keller, R. K., T. P. Arnold, and S. J. Fliesler. 2004. Formation of 7-dehydrocholesterol-containing membrane rafts in vitro and in vivo, with relevance to the Smith-Lemli-Opitz syndrome. *J. Lipid Res.* 45:347–355.
36. Patra, M. 2005. Lateral pressure profiles in cholesterol-DPPC bilayers. *Eur. Biophys. J.* 35:79–88.
37. Cullis, P., and B. De Kruijff. 1978. Polymorphic phase behavior of lipid mixtures as detected by ³¹P NMR. Evidence that cholesterol may destabilize bilayer structure in membrane systems containing phosphatidylethanolamine. *Biochim. Biophys. Acta.* 507:201–218.
38. Simon, S., T. J. McIntosh, and R. Lattore. 1982. Influence of cholesterol on water penetration into bilayers. *Science.* 216:65–68.
39. Chen, Z., and R. P. Rand. 1997. The influence of cholesterol on phospholipid membrane curvature and bending elasticity. *Biophys. J.* 73:267–276.
40. Chernomordik, L., M. M. Kozlov, and J. Zimmerberg. 1995. Lipids in biological membranes fusion. *J. Membr. Biol.* 146:1–14.
41. Malinin, V. S., and B. R. Lentz. 2002. Pyrene cholesterol reports the transient appearance of nonlamellar intermediate structures during fusion of model membranes. *Biochemistry.* 41:5913–5919.
42. Kim, K., C. Kim, and Y. Byun. 2001. Preparation of a dipalmitoyl-phosphatidylcholine/cholesterol Langmuir-Blodgett monolayer that suppresses protein adsorption. *Langmuir.* 17:5066–5070.
43. Worthman, L.-A. D., K. Nag, P. J. Davis, and K. M. W. Keough. 1997. Cholesterol in condensed and fluid phosphatidylcholine monolayers studied by epifluorescence microscopy. *Biophys. J.* 72:2569–2580.
44. Patzer, E. J., R. R. Wagner, and Y. Barenholz. 1978. Cholesterol oxidase as a probe for studying membrane organization. *Nature.* 274:394–395.
45. Holopainen, J. M., A. J. Metso, J.-P. Mattila, A. Jutila, and P. K. J. Kinnunen. 2004. Evidence for the lack of a specific interaction between cholesterol and sphingomyelin. *Biophys. J.* 86:1510–1520.
46. Huang, J., and G. W. Feigenson. 1999. A microscopic interaction model of maximum solubility of cholesterol in lipid bilayer. *Biophys. J.* 76:2142–2157.
47. Huang, J. 2002. Exploration of molecular interactions in cholesterol superlattices: effect of multibody interactions. *Biophys. J.* 83:1014–1025.
48. Davies, J. T., and E. K. Rideal. 1963. *Interfacial phenomena*, 2nd ed. Academic Press, New York.
49. Ipsen, J. H., G. Karlström, O. G. Mouritsen, H. Wennerström, and M. J. Zuckermann. 1987. Phase equilibria in phosphatidylcholine-cholesterol system. *Biochim. Biophys. Acta.* 905:162–172.
50. Veatch, S. L., K. Gawrisch, and S. L. Keller. 2006. Closed-loop miscibility gap and quantitative tie-lines in ternary membranes containing diphytanoyl PC. *Biophys. J.* 90:4428–4436.

51. Hsueh, Y.-W., K. Gilbert, C. Trandum, M. Zuckermann, and J. Thewalt. 2005. The effect of ergosterol on dipalmitoylphosphatidylcholine bilayers: a deuterium NMR and calorimetric study. *Biophys. J.* 88:1799–1808.
52. Mannock, D. A., R. N. A. H. Lewis, and R. N. McElhaney. 2006. Comparative calorimetric and spectrometric studies of the effects of lanosterol and cholesterol on the thermotropic phase behavior and organization of dipalmitoylphosphatidylcholine bilayer membranes. *Biophys. J.* 91:3327–3340.
53. Radhakrishnan, A., and H. M. McConnell. 1999. Cholesterol-phospholipid complexes in membranes. *J. Am. Chem. Soc.* 121:486–487.
54. Harroun, T. A., J. Katsaras, and S. R. Wassall. 2006. Cholesterol hydroxyl group is found to reside in the center of a polyunsaturated lipid membrane. *Biochemistry.* 45:1227–1233.
55. Tu, K., M. L. Klein, and D. J. Tobias. 1998. Constant-pressure molecular dynamics investigation of cholesterol effects in a dipalmitoylphosphatidylcholine bilayer. *Biophys. J.* 75:2147–2156.
56. Czub, J., and M. Baginski. 2006. Comparative molecular dynamics study of lipid membranes containing cholesterol and ergosterol. *Biophys. J.* 90:2368–2382.
57. Rychnovsky, S. D., and D. E. Mickus. 1992. Synthesis of ent-cholesterol, the unnatural enantiomer. *J. Org. Chem.* 57:2732–2736.
58. Rog, T., M. Pasenkiewicz-Gierula, I. Vattulainen, and M. Karttunen. 2007. What happens if cholesterol is made smaller: importance of methyl substituents in cholesterol ring structure on phosphatidylcholine-sterol interaction. *Biophys. J.* 92:3346–3357.
59. Vainio, S., M. Jansen, M. Koivusalo, T. Rog, M. Karttunen, I. Vattulainen, and E. Ikonen. 2006. Significance of sterol structural specificity. Desmosterol cannot replace cholesterol in lipid rafts. *J. Biol. Chem.* 281:348–355.
60. Demel, R. A., W. S. Geurts van Kessel, R. F. Zwaal, B. Roelofsen, and L. L. van Deenen. 1975. Relation between various phospholipase actions on human red cell membranes and the interfacial phospholipid pressure in monolayers. *Biochim. Biophys. Acta.* 406:97–107.